

## Industrial Byproduct- Based Concrete Subjected to Carbonation. Electrochemical Behavior of Steel Reinforcement

Willian Aperador<sup>1,\*</sup>, Rosa Vera<sup>2</sup>, Ana María Carvajal<sup>3</sup>

<sup>1</sup> Departamento de Ingeniería, Universidad Militar Nueva Granada, Carrera 11 No. 101-80, Fax:+57(1) 6343200, Bogotá, Colombia.

<sup>2</sup> Laboratorio de Corrosión, Instituto de Química. Pontificia Universidad Católica de Valparaíso, Avda. Universidad, 330, Placilla, Valparaíso

<sup>3</sup> Escuela de Construcción Civil, Facultad de Ingeniería, Pontificia Universidad Católica de Chile, Av. Vicuña Mackenna 4860, Macul, Santiago

\*E-mail: [g.ing.materiales@gmail.com](mailto:g.ing.materiales@gmail.com)

*Received:* 2 October 2012 / *Accepted:* 11 November 2012 / *Published:* 1 December 2012

---

Samples of ASTM A-706 structural steel embedded in different concretes obtained from mixtures of alkali-activated steel slag and fly ash were exposed to accelerated carbonation under controlled conditions (4% CO<sub>2</sub>, 65% RH and 25°C). Concretes prepared with Ordinary Portland Cement (OPC) (Type I) and Granulated Blast Furnace Slag Cement (GBFS) were used for comparison. Analysis of the electrochemical phenomenon taking place on the surface of the steel due to CO<sub>2</sub> transport through the concrete matrix was performed by measurements of open circuit potential (OCP) and linear polarization resistance (LPR). The steel-concrete interface was characterized using Mössbauer spectroscopy at room temperature and X-ray diffraction (XRD). The electrochemical measurements suggest passivation of the steel in the concretes prepared using mixtures of steel slag and fly ash without cement.

---

**Keywords:** fly ash, steel slag, accelerated carbonation, corrosion.

### 1. INTRODUCTION

New engineering materials aim to satisfy all and any mechanical requirements, along with cost and design requirement, while leading to lower environmental impact during their production or use. With the increase in the global construction industry and the desire to offer increasingly more economic materials which contribute to protecting the environment, the development of alternative materials has begun to look to produce cement and concrete with mechanical performance and durability that are over and above those of traditional concrete [1-4].

The use of two industrial byproducts (steel slag (GBFS) and fly ash (FA) from steel foundries and thermoelectric stations, respectively) would represent an important advancement in innovation in process technology and in the development of construction materials as alternatives to traditional Portland cement (OPC) [5-6]. Ideally, these alternatives would not lead to pollutant gas emissions during their manufacture, should provide notable energy savings and increase the useful life of buildings [7]. All of these aspects would promote the development of new industries and the possibility for greater competition in certain markets.

Steel slag and fly ash are two byproducts from the Colombian industrial sector with the highest potential for use as raw materials in alternative technology concrete production, with their transformation and preparation leading to lower energy consumption than with traditional Portland concretes. In this study the two byproducts were used as substitute cement material, and can be activated to accelerate hydration of the steel slag and the fly ash. Previous studies have demonstrated that both byproducts mixed separately with Portland cement show improved mechanical compressive strength, a denser structure and good levels of durability compared to Portland cement alone [8-10]. However, their properties against corrosion and their potential application as a construction material have not been assessed.

Steel embedded in concrete is normally in a passive state; however, the pH of concrete can be altered by the incorporation of different substances from the environment. These are mainly CO<sub>2</sub>, which is in the air, and SO<sub>3</sub>, which is found in industrial environments. In highly polluted areas with high levels of rainfall, pH can reach up to 4. This is commonly known as acid rain and can affect concrete structures in the same way as carbonation. Carbonation of concrete describes the loss of basicity due to acidic pollution [11]. Carbonation occurs with greater frequency in urban areas, which have high concentrations of sulfuric oxides (SO<sub>x</sub>) and nitrous oxides (NO<sub>x</sub>), which in turn combine with the water in the atmosphere, forming the respective sulfurous and nitrous acids, and later sulfuric acid and nitric acid.

The objective of this study is to determine the electrochemical behavior of a steel rebar embedded in alternative concrete prepared using steel slag and fly ash (GBFS-FA), without any commercial cement, when subjected to normal atmospheric conditions and conditions of 4% CO<sub>2</sub>. The values obtained were compared with those from concrete based on OPC and GBFS exposed to the same aggressive conditions.

## 2. MATERIALS AND METHODS

### 2.1 Concrete samples and specimen preparation

Type F fly ash (FA) from the Termozipa thermoelectric station was used in this study. Table 1 shows the chemical composition of the fly ash. Calcination loss was determined by calcining the sample at 1000 °C. The result obtained was 4.23% of the total mass; which is mainly attributed to unburned carbon remnants. The silica percentage of the fly ash was also determined in accordance with the procedure described in standard UNE 80-225-93, giving a value of 41.23% in mass.

The other substitute material used was steel slag (GBFS) from a blast furnace in Colombia, with a chemical composition as shown in Table 1. The coefficient of basicity ( $\text{CaO}+\text{MgO}/\text{SiO}_2+\text{Al}_2\text{O}_3$ ) and that of quality ( $\text{CaO}+\text{MgO}+\text{Al}_2\text{O}_3/\text{SiO}_2+\text{TiO}_2$ ) are 1.0 and 1.73, respectively. A sodium silicate solution at a concentration of 5%  $\text{Na}_2\text{O}$  expressed as a percentage of slag weight was used as alkali-activator.

The aggregates used were gravel with a maximum size of 17 mm, specific gravity of 3.12 and absorption of 1.6%, and river sand with specific surface area of  $2380 \text{ kg m}^{-3}$  and absorption of 3.0%.

These materials were used to prepare concrete with 400 kg of cementing material per  $\text{m}^3$  of concrete, with a water/cement ratio of 0.40.

**Table 1.** Chemical composition of the fly ash and steel slag used as cement.

Composition	Fly ash (% mass)	Steel slag (% mass)
$\text{SiO}_2$	56.6	33.7
$\text{Al}_2\text{O}_3$	23.1	12.8
$\text{Fe}_2\text{O}_3$	4.6	0.48
$\text{CaO}$	5.7	45.4
$\text{MgO}$	0.9	1.0
$\text{Na}_2\text{O}$	0.8	0.12
$\text{K}_2\text{O}$	1.4	1.5
$\text{P}_2\text{O}_5$	0.7	-
$\text{TiO}_2$	1.0	0.5
$\text{MnO}$	0.01	-
$\text{SO}_3$	0.50	-
$\text{SiO}_2/\text{Al}_2\text{O}_3$	2.7	2.63

Samples of Portland concrete (OPC) and concrete using steel slag cement (GBFS) were also prepared for this study for reference purposes. In addition, further concrete samples were prepared using alkali-activated steel slag with different percentages of fly ash: 10% (90% slag and 10% fly ash) and 20% (80% slag and 20% fly ash).

## 2.2 Electrochemical testing

In order to take electrochemical measurements, concrete cylinders 76.2 mm in diameter and 76.2 mm high were prepared with a rebar made of ASTM A706 structural steel [12] in the center of the test probe; the steel rebar had a diameter of 6.35 mm, as shown in Figure 1. As can also be seen in this figure, the length of the exposed steel was 50 mm. The concrete prepared with slag cement and with mixtures of steel slag with 10% and 20% fly ash were cured at a relative humidity of 90%, and the OPC cement at a relative humidity of 100%. The specimens were exposed in the carbonation chamber 28 days after their preparation.

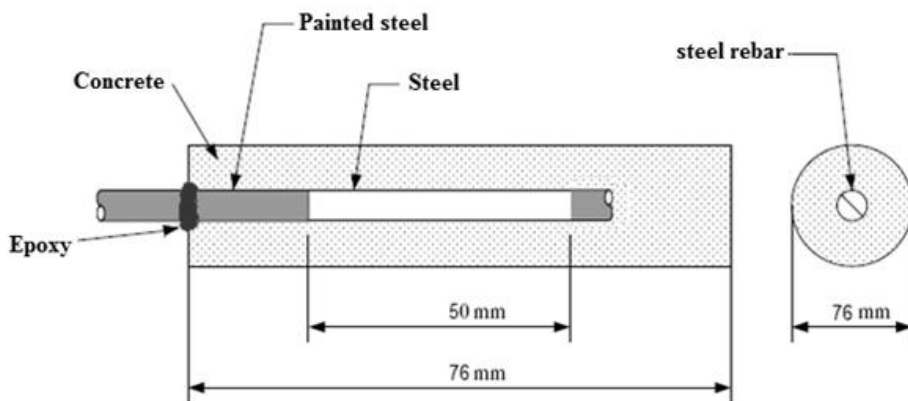


**Figure 1.** Design of the reinforced concrete sample.

Electrochemical characterization was performed under immersion in a solution of distilled water, using a Gamry PCI 4 potentiostat/galvanostat. Measurements were taken of open circuit potential and linear polarization resistance using a cell comprising a graphite counter-electrode, a Cu/CuSO<sub>4</sub> reference electrode and the ASTM A706 structural steel as the working electrode with an exposed area of 10 cm<sup>2</sup> (Figure 2).

The linear polarization resistance (LPR) testing was performed with an external potential variation ( $\pm 20\text{mV}$ ) around the open circuit potential. Measurements of open circuit potential were taken at 12,000 seconds until stabilization was reached.

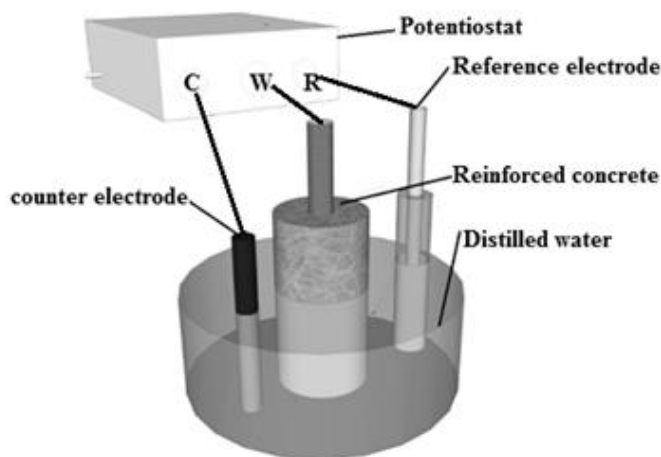


**Figure 2.** Experimental set-up for electrochemical measurements.

Measurement of the advancement of the corrosion resulting from the incorporation of carbon dioxide was done in a carbonation chamber under controlled conditions (4% CO<sub>2</sub>, 65% relative humidity and a temperature of 25 °C). The evaluation time for each of the probes was 0, 350, 700, 1050, 1400, 2000 and 2600 hours.

The pH level measured in the structure after 2600 hours of exposure to the carbonation chamber was measured in the pore solution in accordance with the in situ leeching technique proposed by Sagues et al. [13].

### 2.3 Characterization of corrosion products

X-ray diffraction (XRD) was used to identify the corrosion products formed on the steel surface. The equipment used was a PW3050/60 ( $\theta/\theta$ ) goniometer, managed under an XPERT-PRO system using monochromatic Cu K $\alpha$  radiation 1.54 Å, operating at 40kV and 40 mA at a temperature of 25°C. The surface sweep was performed from  $2\theta = 20.01^\circ$  to  $2\theta = 99.99^\circ$  with a step of  $2\theta = 0.02^\circ$  at a scan time of 1 second. The crystalline phases of the steel surface were determined using an XPERT-PRO X-ray diffractometer, applying the device's diffraction database. The MAUD program was also used on the basis of the Rietveld method. This method consists of fitting a theoretical diagram to coincide fully with what has been observed. These theoretical diagrams are obtained from crystalline structures and a series of crystalline parameters. The phases that were found in this study contrast with those reported by other researchers [14]. Mössbauer spectra were used to analyze the phases; they were measured using a typical arrangement of  $^{57}\text{Fe}$  Mössbauer spectrometry. A tablet of  $^{57}\text{Co}$  in a rhodium matrix was used as the Mössbauer source, which decays radioactively into  $^{57}\text{Fe}$ . As the radioactive process of the source of  $^{57}\text{Co}$  emits different types of radiation, this gives the possibility of two different modes of use for Mössbauer spectroscopy, transmission and reflection, each of which provides different information; in this study Transmission Mössbauer Spectroscopy (TMS) was used [15].

The morphology of the corrosion products was evaluated using a high resolution scanning electron microscope (Philips XL 30 FEG) fitted with a light sensitive element (EDX system) and with a resolution of 1-nm in 30 kV.

## 3. RESULTS

### 3.1 Corrosion potential

The graph in Figure 3 demonstrates the corrosive phenomenon occurring on the concretes with ordinary Portland cement (OPC) and steel slag cement (GBFS) and the GBFS/FA mixtures, evaluated thermodynamically taking into account the criteria of standard ASTM C876-91 [16]. Since the type of material in which the steel is embedded is different, the systems present different values for rest potential. The probes prepared with mixtures of activated slag and fly ash (GBFS 90% + FA 10%) and (GBFS 80% + FA 20%), i.e. without cement, show passivation behavior when under a process of accelerated carbonation; this maintains until the end of the evaluation.

The concrete probes prepared with slag cement and subjected to accelerated carbonation suggest the existence of active corrosion in the steel, generated from the beginning of exposure. This loss of passivation and generation of active corrosion stabilizes at 2000 h, and continues until the end

of the evaluation. From the analysis of corrosion potential of the ordinary Portland concrete, it can be seen that the potential increases from 0 to 1400 hours, showing the passivity of the steel, later beginning to lose passivity with a higher probability of corrosion at 2000 hours. The fall in corrosion potential of the steel continues with the carbonation process of the concrete. At 2600 hours active corrosion can be seen, thus destroying the passivation layer [17-18].

For the OPC concrete probes, the initial pH of the mixture was 13.4, while after carbonation it was 9.7 and 10.2. For the GBFS, the initial pH was 14 and between 8.2 and 8.9 after the carbonation process. For the mixtures, the initial pH was at 13.8, while at the end of the carbonation test, the pH had reached between 10.2 and 11.3. These results corroborate the corrosion behavior of steel in different mixtures by the end of the carbonation testing.

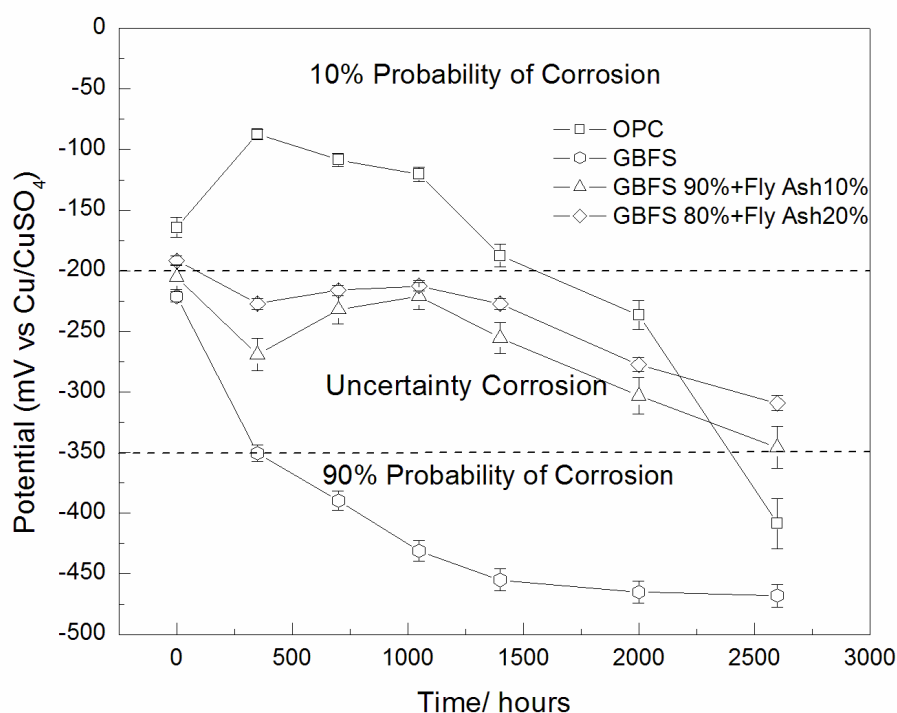


**Figure 3.** Corrosion potential ( $E_{corr}$ ) over time, for steel rebars embedded in concretes prepared with GBFS, OPC, 90% GBFS+10% FA and 80% GBFS+20% FA, exposed to accelerated carbonation.

### 3.2 Polarization Resistance

Figure 4 shows the polarization resistance values for the slag concrete, indicating that the concrete exposed to accelerated  $CO_2$  conditions generates a fall in corrosion resistance along with the increase in carbonation. When carbonation reaches 100% of the probe, a value of  $21 \text{ k}\Omega \text{ cm}^2$  is obtained, which is 6 times less than at 0 hours ( $120 \text{ k}\Omega \text{ cm}^2$ ). This can be attributed to the reduction in pH, the decalcification of hydrated calcium silicates and a subsequent increase in porosity [7]. The high carbonation rate exhibited by GBFS concrete may be attributed to the fact that the characteristic activation reactions after slag alkali activation are governed by dissolution and precipitation

mechanisms, whose reaction kinetics are faster than the diffusion reactions that prevail in OPC hydration [19-20]. When dissolved species such as calcium, silicates and aluminates reach the maximum concentration they can precipitate, prompting the nucleation of the dissolved aluminates and silicates in an alkaline environment. This would favour the formation of a C-S-H gel characterized by a short range order due to its low Ca/Si ratio and the presence of Q<sup>3</sup>-type Si units [21]. It has been pointed out that CO<sub>2</sub> reacts directly with the C-S-H gel in these materials leading to its decalcification and a loss of cohesion in the matrix [22], and it has been suggested that this unsuitability could be attenuated by grinding the slag much more finely and enhancing the efficiency of curing systems, proposing airtight systems with an average RH of around 90% [23].

For the OPC under the same conditions, the polarization resistance value increases until 1050 hours, reaching a value of 2980 kΩ cm<sup>2</sup>, while at 2500 hours when 100% carbonation is achieved, a sharp fall is seen to a value of 162 kΩ cm<sup>2</sup>. As a consequence, the passive layer has begun to generate a degradation process, though the value at 2600 h is higher than that found for the slag concrete when 100% carbonation is reached.

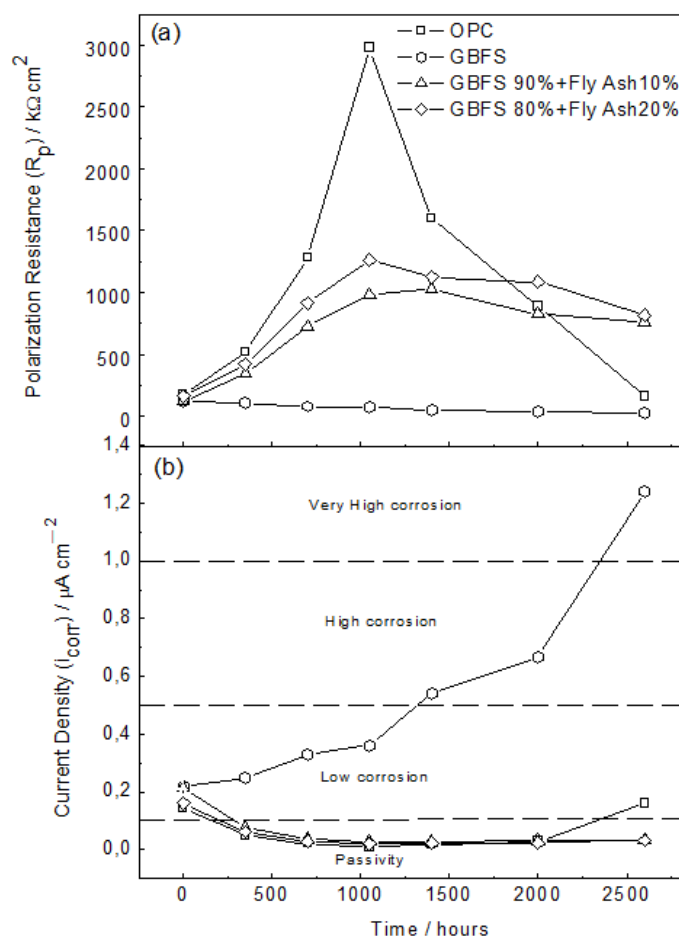


**Figure 4.** Polarization resistance ( $R_p$ ) and current density ( $i_{corr}$ ) over time for steel rebars embedded in GBFS, OPC, 90%GBFS+10%FA and 80%GBFS+20%FA concretes with exposure to carbonation.

For the concretes prepared with mixtures of alkali-activated steel slag with 10% or 20% fly ash, polarization resistance increases as a function of exposure time, reaching a value of  $1025 \text{ k}\Omega \text{ cm}^2$  at 1400 hours for the concrete with 10% fly ash, while for the concrete with 20% fly ash the value is higher at 1050 hours ( $1263 \text{ k}\Omega \text{ cm}^2$ ). This suggests that the concrete with 20% fly ash generates a greater passive layer, though in both concretes the steel remains passive throughout. These results correlate with those for potential shown in Figure 3.

After 2600 hours of carbonation it can be seen that of the mixtures with new cementing materials, the highest level of polarization resistance is the concrete with 80% GBFS and 20% FA. This may be due to the good formation of a protective layer on the steel surface as a result of the presence of alkaline species, such as KOH, NaOH and  $\text{Ca}(\text{OH})_2$ . At the same time the pores in this concrete are blocked by these same species, which helps the generation of a good level of polarization resistance [24-25].

### 3.3 Characterization of corrosion products

XRD analysis of the surfaces of the steel rebars embedded in the different concretes for a period of 2600 hours demonstrates the present of iron oxides and hydroxides on all the samples (the OPC, GBFS concretes and the mixtures of 90%GBFS+10%FA and 80%GBFS+20%FA). Other components that appear in the XRD analysis are attributed to the aggregates and cementing materials.

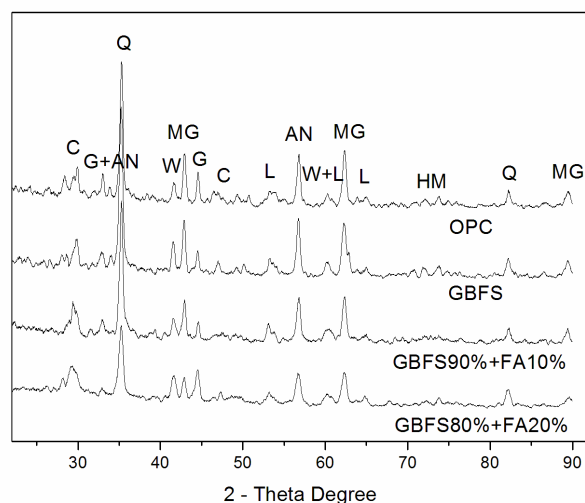


**Figure 5.** XRD for steel rebars embedded in GBFS, OPC, 90%GBFS+10%FA and 80%GBFS+20%FA concretes with exposure to carbonation.

The upper part of Figure 5 shows the XRD spectra of the alkali-activated steel slag concrete exposed to accelerated carbonation, showing presence of the following phases: C: calcite, G: goethite, AN: Andradite, MG: magnetite, W: wüstite, L: lepidocrocite, HM: hematite and Q: quartz. The Q phase shows high intensity, which is attributed to the concrete matrix (cementing material and aggregates). The oxides found on the steel surface are MG and W; it can be seen that these phases have

highest intensity in comparison with the others, excluding quartz. The hydroxides found are G, L and HM. Both the oxides and hydroxides seen in these spectra are those found in most corrosion processes associated with steel embedded in OPC concrete and in 90%GBFS +10%FA and 80%GBFS +20%FA concrete, though with generally lower intensity.

Figure 6 shows the Mössbauer spectra at room temperature for the different specimens. In order to obtain the best fit of the Mössbauer spectra for the samples of OPC, GBFS, 90%GBFS + 10%FA and 80%GBFS + 20%FA exposed to accelerated carbonation for 2600 hours in a carbonation chamber, three sextets and two duplicates were used for all concrete types. Two of the sextets were fitted using hyperfine magnetic fields (Bf) 48.3 and 45.9 T, quadrupole splitting ( $\Delta$ ) zero for both, isomeric deviations ( $\delta$ ) between 0.16 and 0.57 mm/s, respectively, and are attributed to a spinel magnetite phase ( $Fe_{3-x}O_4$ ) or a possible combination of  $Fe_{3-x}O_4$  / maghemite ( $\gamma-Fe_2O_3$ ). The remaining sextet was fitted with parameters Bf = 28.5 T,  $\Delta = -0.019$  mm/s and  $\delta = 0.06$  mm/s, and attributed to a Fe phase. For one of the duplicates, values of  $\Delta = 1.17$  mm/s and  $\delta = 0.05$  mm/s were found, which correspond to the presence of  $Fe^{2+}O$ ; while for the other duplicate, the value of  $\Delta = 0.72$  mm/s and  $\delta = 0.83$  mm/s were identified, corresponding to the presence of  $Fe^{3+}O(OH)$ .

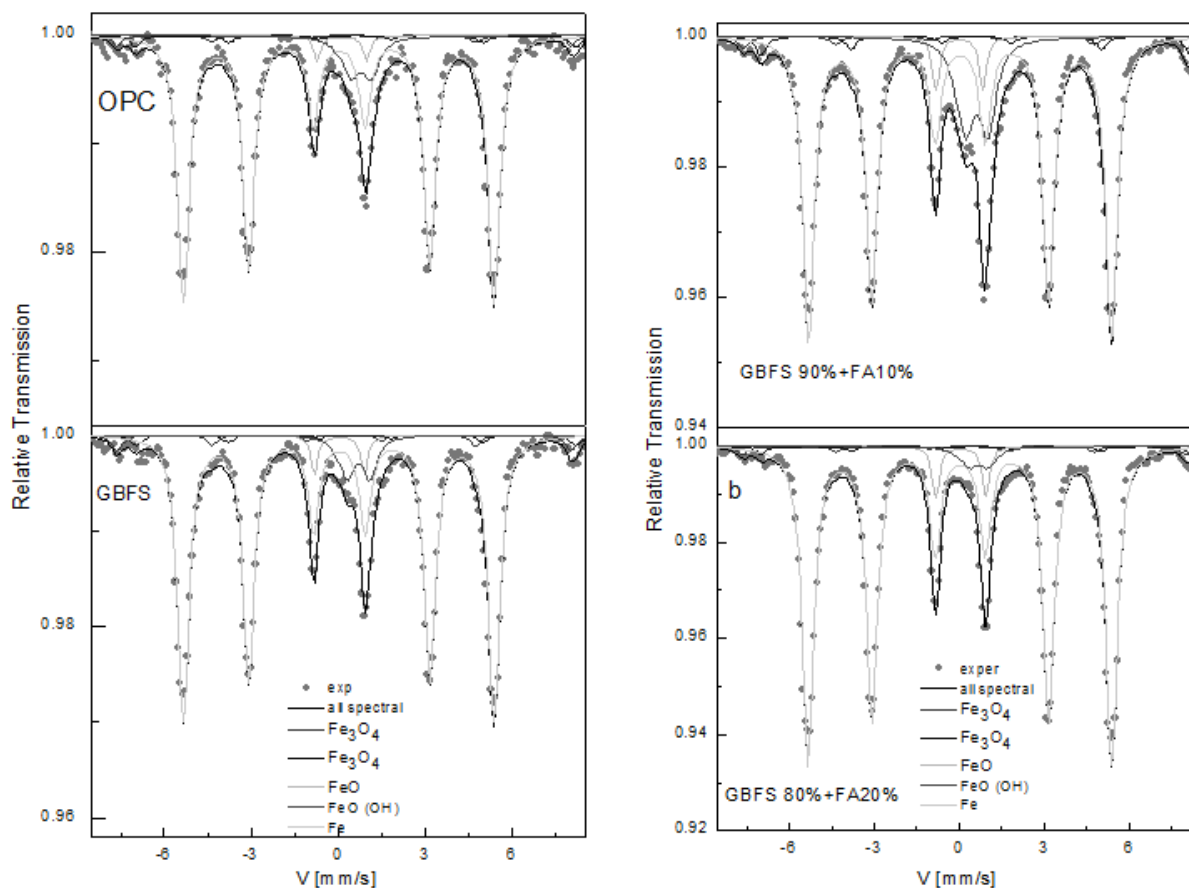


**Figure 6.** Mössbauer Spectra for the OPC, GBFS, 90%GBFS+10%FA and 80%GBFS+20%FA concretes exposed to accelerated carbonation.

Table 2 details the results for oxide and hydroxide percentages present in each concrete type. It can be seen that there is a high percentage of iron in all cases. For the 90%GBFS+10%FA and 80%GBFS+20%FA concretes the proportion of goethite hydroxide is higher compared to the other products found (Magnetite and Wüstite), suggesting that the majority of products found are Goethite. The percentages of corrosion products on the steel embedded in the 90%GBFS+10%FA and 80%GBFS+20%FA concretes are approximately similar to each other, with only an increase in the Goethite phase seen with the higher proportion of alkaline slag.

**Table 2.** Relations of areas of the Mössbauer spectrum to the products found for the OPC, GBFS, 90%GBFS+10%FA and 80%GBFS+20%FA concretes exposed to accelerated carbonation.

Phase (%)	OPC	GBFS	90%GBFS +10%FA	80%GBFS +20%FA
Magnetite	5.75±0.0011	6.60±0.0016	4.13±0.0011	3.29±0.0014
Wüstite	2.31±0.0023	3.71±0.0012	2.58±0.0021	3.35±0.0026
Goethite	8.72±0.0043	12.68±0.0028	4.65±0.0029	3.46±0.0032
Iron	83.22±0.0018	77.01±0.0019	88.64±0.0010	89.9±0.0021

Wüstite is stable only at high temperatures. Therefore, at room temperature it appears in the form of a sheet of residue offering very little protection in the long term for the steel exposed to accelerated carbonation. The Goethite has a high percentage due to dissolution and precipitation of Lepidocrocite, which transforms into goethite, since no Lepidocrocite appears in the Mössbauer spectrum [13].

The information gathered by the XRD and Mössbauer methods are analogous since on the steel rebar surface embedded in different concrete types, the presence of iron oxides and hydroxides was found in the samples, also identifying the formation of Magnetite ( $\text{Fe}_3\text{O}_4$ ), Wüstite ( $\text{Fe}^{2+}\text{O}$ ) and Goethite ( $\text{Fe}^{3+}\text{O}(\text{OH})$ ) as the main corrosion products. Other products such as Lepidocrocite and Hematite were found at lower levels of intensity, possibly due to the low percentage of these hydroxides present in the samples, and to the mixture with iron as they possess similar parameters.

### 3.4 SEM Analysis

Figure 7 shows the SEM micrographs of the corrosion products deposited on the surface of steel rebars embedded in the 90%GBFS+10%FA concrete subjected to accelerated carbonation. Figure 7a shows that the corrosion products (Magnetite, Goethite and Wüstite) are overlaid, showing an area labeled homogeneous due to the absence of cracks. In the amplified area, a crack can be seen generated by the movement of the corrosion products, as the products diverge from all areas and there is a space at the point where they meet. Magnifying the areas labeled in Figure 7b (Figure 7c), an area is found where there is the highest concentration of cracks. The dark areas are associated with magnetite due to their apparent morphology. These dark areas are generated by the higher concentration of cracks due to

the dilation of magnetite. Based on this micrograph it can be said that the first layer formed on the steel is the magnetite and that the following layer results from the formation of corrosion products during the development of the process. In the magnification shown in Figure 7d, the corrosion products on the external surface can be seen. These products are Goethite and Wüstite, the formation of which is in line with the findings of the XRD and Mössbauer analyses. The layer observed shows greater homogeneity over the layer found on the steel surface, due to the appearance of a lower concentration of cracks.

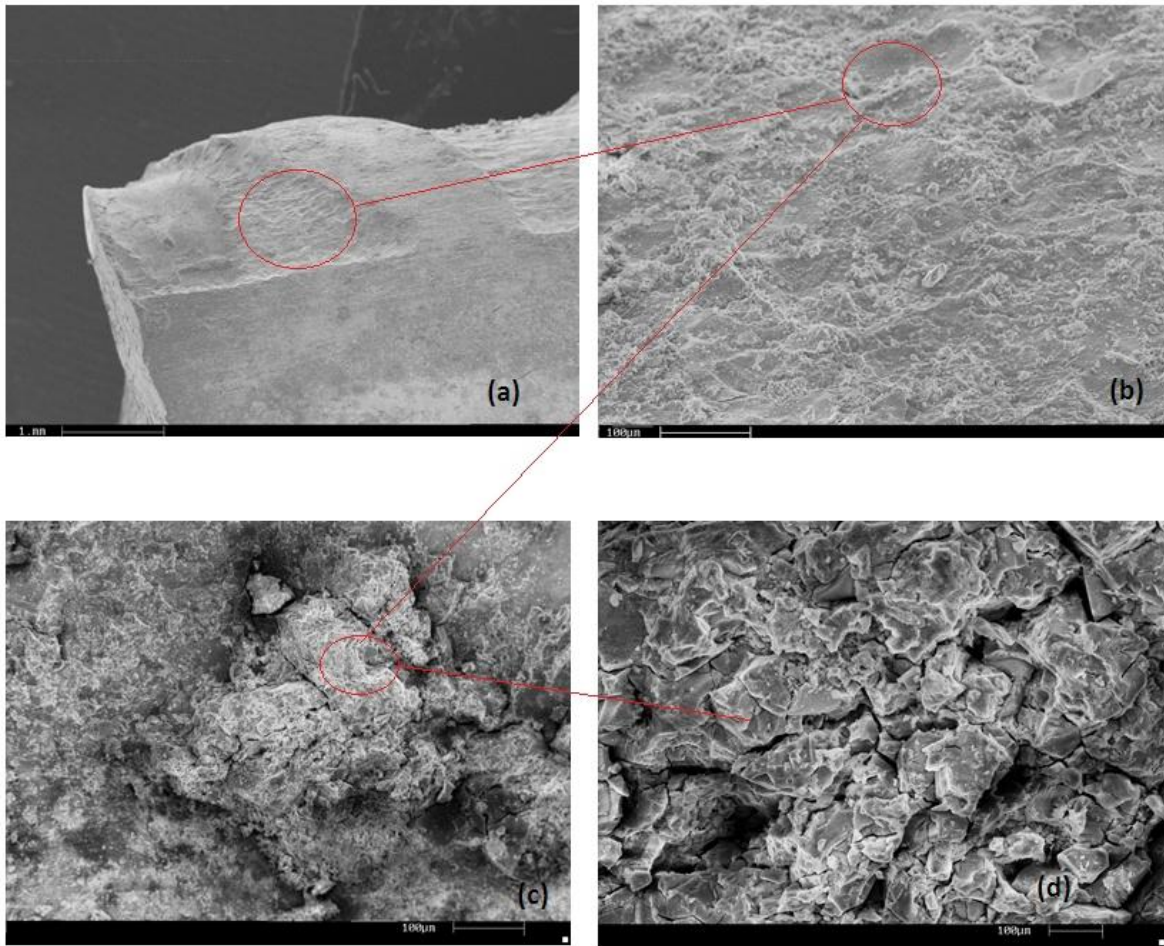


**Figure 7.** SEM of the corrosion products deposited in the steel embedded in concrete 90% GBFS +10% FA.

#### 4. CONCLUSIONS

The concretes prepared with mixtures of alkali-activated steel slag and fly ash subject to accelerated carbonation show lower susceptibility to the carbonation process in comparison with concretes prepared with OPC and GBFS. The corrosion potential,  $E_{corr}$ , stabilizes at the beginning of the process, indicating that the steel rebar embedded in the GBFS + FA concrete is in a state of inactive corrosion during evaluation under the study conditions.

The polarization resistance corroborates the information obtained for Ecorr measurements, where the GBFS+FA concretes show increased polarization resistance for the steel in the first hours until 1050 hours carbonation, later falling. However, using the criteria for current density, a passive state is maintained throughout. For the GBFS concrete under the same conditions, there is a fall in each of the studied levels, suggesting that the deterioration of the steel bar continues.

The steel embedded in OPC, GBFS, 90%GBFS+10%FA and 80%GBFS+20%FA concrete and exposed to the carbonation process show the presence of iron oxides and hydroxides. For all samples, the corrosion products included Magnetite ( $\text{Fe}_3\text{O}_4$ ), Wüstite ( $\text{Fe}^{2+}\text{O}$ ) and Goethite ( $\text{Fe}^{3+}\text{O}(\text{OH})$ ). The steel embedded in the OPC and GBFS concretes shows increased formation of corrosion products in comparison with the steel in the GBFS+FA concretes.

Based on the electrochemical properties and surface evaluation of the steel embedded in the concrete prepared with alkali-activated steel slag and fly ash subject to accelerated carbonation, it can be seen that the GBFS+FA concretes show lower corrosion product generation due to lower  $\text{CO}_2$  permeability, generating lower pore interconnection.

#### ACKNOWLEDGEMENTS

The authors of this study express their appreciation to the Research Department of the Universidad Militar Nueva Granada for financing received.

#### References

1. C. Shi C., *Cement Concrete Res.* 26 (1996) 1789.
2. A. Fernández-Jimenez, F. Puertas, *Advances In Cements Research* 15 (2003) 129.
3. A. Fernández-Jiménez, A. Palomo, *Revista Ingeniería de Construcción* 24 (2009) 213.
4. W. Aperador, D. M. Bastidas, J. Bautista, *Rev. Fac. Ing. Univ. Antioquia* 62 (2012) 189.
5. E. Rodríguez, S. Bernal, R. Mejía de Gutiérrez, F. Puertas, *Mater. Construc.* 58 (2008) 53.
6. S. D. Wang, K. L. Scrivener, *Cement Concrete Res* 25 (1995) 561.
7. M. Palacios, F. Puertas, *J. Am. Ceram. Soc.* 89 (2006) 3211.
8. J. E. Oh, P. J. Monteiro, S. S. Jun, S. Choi S, S. M. Clark, *Cement Concrete Res.* 40 (2010) 189.
9. M. Komljenović, Z. Bašćarević, V. Bradić, *J. Hazard. Mater.* 181 (2010) 35.
10. M. Criado, A. Fernández Jiménez, A. Palomo, *Cement Concrete Comp.* 32 (2010a) 589.
11. W. Aperador W., R. Mejía de Gutiérrez, D. M. Bastidas, *Corros Sci.* 51 (2009) 2027.
12. ASTM A 706-08 Standard, Standard specification for low-alloy steel deformed and plain bars for concrete reinforcement, West Conshohocken, PA, American Society for Testing and Materials, 2008.
13. A. Sagüess, M. A. Pech- Canul, A. K. M. Shahid Al- Mansur, *Corros. Sci.* 45 (2003) 7.
14. W. Aperador, J. Bautista, E. Vera, *Dyna* 170 (2011) 198.
15. R. R. Rodríguez, G. A. Pérez-Alcáraz, H. Sánchez, J. M. Greneche, *Microelectron J* 39 (2008) 1311.
16. ASTM C 876-99 Standard, Standard test for half-cell potentials of uncoated reinforcing steel in concrete, West Conshohocken, PA, American Society for Testing and Materials, 1999.
17. D. M. Bastidas, A. Fernández-Jiménez, J. A. Palomo, J. A. González, *Corros. Sci.* 50 (2008) 1058.
18. G. Blanco, A. Bautista, H. Takenouti, *Cement and Concrete Composites*, 28 (2006) 212.
19. F. Puertas, M. Palacios, T. Vázquez, *J Mater Sci*, 41 (2006) 3071.

20. A. Fernández-Jimenez, A.G. de la Torre, A. Palomo, G. López-Olmo, M.M. Alonso, M.A.G. Aranda. *Fuel*, 85 (2006) 625.
21. H.-W. Song, V. Saraswathy. *J. Hazard. Mater*, 138 (2006) 226.
22. M. Criado, A. Palomo, A. Fernández-Jiménez, *Fuel*, 84 (2005) 2048.
23. V. Živica. *Constr. Build. Mater*, 21 (2007) 1463.
24. R. Montoya, W. Aperador, D.M. Bastidas. *Corrosion Sci*, 51 (2009) 2857.
25. C. Andrade, V. Castelo, C. Alonso, J. González (1984), "Determination of the corrosion rate of steel embedded in concrete by the polarization resistance and ac impedance methods" ASTM-STP 906, ASTM, Philadelphia, PA, 43-63.